

Multilayer Hybrid Microfluidics: A Digital-to-Channel Interface for Sample Processing and Separations

Michael W. L. Watson,[†] Mais J. Jebrail,[†] and Aaron R. Wheeler^{*,†,‡,§}

Department of Chemistry, University of Toronto, 80 St. George Street, Toronto, Ontario, M5S 3H6, Institute of Biomaterials and Biomedical Engineering, University of Toronto, 164 College Street, University of Toronto, Toronto, Ontario, M5S 3G9, and Banting and Best Department of Medical Research, University of Toronto, 112 College Street, Toronto, Ontario, M5G 1L6

Microchannels can separate analytes faster with higher resolution, higher efficiency and with lower reagent consumption than typical column techniques. Unfortunately, an impediment in the path toward fully integrated microchannel-based laboratories-on-a-chip is the integration of pre-separation sample processing. In contrast, the alternative format of digital microfluidics (DMF), in which discrete droplets are manipulated on an array of electrodes, is well-suited for carrying out sequential chemical reactions such as those commonly employed in proteomic sample preparation. We recently reported a new paradigm of “hybrid microfluidics,” integrating DMF with microchannels for in-line sample processing and separations. Here, we build on our initial efforts, introducing a second-generation hybrid microfluidic device architecture. In the new multilayer design, droplets are manipulated by DMF in the two-plate format, an improvement that facilitates dispensing samples from reservoirs, as well as droplet splitting and storage for subsequent analysis. To demonstrate the capabilities of the new method, we implemented an on-chip serial dilution experiment, as well as multistep enzymatic digestion. Given the myriad applications requiring preprocessing and chemical separations, the hybrid digital-channel format has the potential to become a powerful new tool for micro total analysis systems.

Microchannels have revolutionized separation science, allowing for rapid, efficient analyses with miniscule reagent and sample consumption.¹ To complement chemical separations, microchannel-based systems have been developed incorporating precolumn reactions, including enzymatic digestion,² organic synthesis,³ and fluorescent derivatization.^{4,5} These techniques represent the

promise of the “lab-on-a-chip.” Unfortunately, the scope of laboratories-on-a-chip capable of integrating precolumn reactions with separations is limited. For example, there are no microchannel-based methods reported that are useful for shotgun proteomics, in which samples are subjected to a rigorous, multistep processing regimen requiring several days to complete.⁶ This deficit is largely mechanistic—managing multiple reagents with precise control over position and reaction time in microchannels is complicated by the near-universal effects of hydrostatic and capillary flows.^{7–9} On-chip microvalves¹⁰ offer some relief from this problem; however, the complicated fabrication and control infrastructure required for this technology limits their widespread adoption and use.¹¹ Another technique that might be useful for precolumn reactions and separations is multiphase microchannel systems (i.e., droplets-in-channels).¹² Several groups^{13–15} recently reported methods capable of delivering droplets from such systems directly into separation channels. This is an exciting development, but we posit that the droplets-in-channels paradigm is not ideally suited for controlling multistep chemical reactions between many different reagents (as is required for shotgun proteomics⁶), as the droplets in such systems (regardless of their contents) are controlled in series.

An alternative miniaturized fluid handling format to microchannels is digital microfluidics (DMF), a technique in which discrete fluidic droplets are manipulated by electrostatic forces on an array of electrodes coated with an insulating dielectric.^{16–18}

* To whom correspondence should be addressed. Phone: 416-946-3864. Fax: 416-946-3865. E-mail: aaron.wheeler@utoronto.ca.

[†] Department of Chemistry, University of Toronto.

[‡] Institute of Biomaterials and Biomedical Engineering.

[§] Banting and Best Department of Medical Research.

- (1) Chiou, P. Y.; Chang, Z.; Wu, M. C. *J. MEMS* **2008**, *17*, 133–138.
- (2) Gottschlich, N.; Culbertson, C. T.; McKnight, T. E.; Jacobson, S. C.; Ramsey, J. M. *J. Chromatogr., B* **2000**, *745*, 243–249.
- (3) Brivio, M.; Fokkens, R. H.; Verboom, W.; Reinhoudt, D. N.; Tas, N. R.; Goedbloed, M.; Berg, A. v. d. *Anal. Chem.* **2002**, *74*, 3972–3976.
- (4) Jacobson, S. C.; Hergenroder, R.; Moore, A. W., Jr.; Ramsey, J. M. *Anal. Chem.* **1994**, *66*, 4127–4132.
- (5) Ro, K. W.; Lim, K.; Kim, H.; Hahn, J. H. *Electrophoresis* **2002**, *23*, 1129–1137.

(6) Washburn, M. P.; Wolters, D.; Yates, J. R., III *Nat. Biotechnol.* **2001**, *19*, 242–247.

(7) Crabtree, H. J.; Cheong, E. C. S.; Tilroe, D. A.; Backhouse, C. *J. Anal. Chem.* **2001**, *73*, 4079–4086.

(8) Sinton, D.; Li, D. *Colloids Surf., A* **2003**, *222*, 273–283.

(9) Burst, M.; Walker, M.; Bethell, D.; Schiffrin, D. J.; Whyman, R. *J. Chem. Soc. Commun.* **1994**, 801–802.

(10) Unger, M. A.; Chou, H. P.; Thorsen, T.; Scherer, A.; Quake, S. R. *Science* **2000**, *288*, 113–116.

(11) Roman, G. T.; Kennedy, R. T. *J. Chromatogr., A* **2007**, *1168*, 170–188.

(12) Teh, S. Y.; Lin, R.; Hung, L. H.; Lee, A. P. *Lab Chip* **2008**, *8*, 198–220.

(13) Edgar, J. S.; Pabbati, C. P.; Lorenz, R. M.; He, M.; Fiorini, G. S.; Chiu, D. T. *Anal. Chem.* **2006**, *78*, 6948–6954.

(14) Roman, G. T.; Wang, M.; Shultz, K. N.; Jennings, C.; Kennedy, R. T. *Anal. Chem.* **2008**, *80*, 8231–8238.

(15) Niu, X. Z.; Zhang, B.; Marszalek, R. T.; Ces, O.; J. B. Edl, J. B.; Klug, D. R.; de Mello, A. J. *Chem. Commun.* **2009**, 6159–6161.

(16) Wheeler, A. R. *Science* **2008**, *322*, 539–540.

(17) Pollack, M. G.; Fair, R. B.; Shenderov, A. D. *Appl. Phys. Lett.* **2000**, *77*, 1725–1726.

(18) Lee, J.; Moon, H.; Fowler, J.; Schoellhammer, T.; Kim, C.-J. *Sens. Actuators, A* **2002**, *95*, 259–268.

(a) Side-on (Previous Work ²⁴)		(b) Multi-Layer (New Design)	
Property	Effect	Property	Effect
1. Single-plate droplet actuation configuration	<ul style="list-style-type: none"> ➢ No dispensing from reservoirs or splitting droplets ➢ Large errors caused by pipetting ➢ Evaporation problems 	1. Two-plate droplet actuation configuration	<ul style="list-style-type: none"> ➢ Dispensing from reservoirs and droplet splitting ➢ Pipetting errors made negligible ➢ Evaporation limited
2. PDMS device construction	<ul style="list-style-type: none"> ➢ Easy to fabricate ➢ Undesirable surface properties (i.e., surface adsorption of analytes, solvent incompatibility etc.) 	2. Glass device construction	<ul style="list-style-type: none"> ➢ More difficult to fabricate ➢ Superior material properties (i.e., reduced analyte adsorption, solvent compatible etc.)
3. Shared digital and channel substrate	<ul style="list-style-type: none"> ➢ Limited space for electrodes 	3. Separate digital and channel substrates	<ul style="list-style-type: none"> ➢ Larger space for electrodes

Figure 1. Comparison of the side-on hybrid microfluidic device configuration²⁴ and the new multilayer hybrid microfluidic device configuration. (a) The side-on configuration comprises a one-plate digital microfluidic device mated to a PDMS microchannel on a common substrate. The design is straightforward to fabricate; however, it suffers from the requirement of dispensing by pipet and material limitations of PDMS. (b) The new multilayer device design comprises a DMF array patterned on a top substrate mated to a network of microchannels in a glass substrate, below. Although more complex to fabricate, this configuration allows for dispensing droplets from reservoirs and splitting droplets on-chip, and in addition glass is more favorable for microchannel separations.

DMF is well-suited for carrying out sequential chemical reactions; this is particularly true for the two-plate format, in which droplets are sandwiched between a top substrate bearing a ground electrode and a bottom substrate bearing driving electrodes. In this configuration, droplets containing different reagents can be dispensed from reservoirs, moved, merged, mixed, and split,¹⁹ which facilitates multistep proteomic sample processing in which protein samples are sequentially reduced, alkylated, and digested prior to mass spectrometric analysis.^{20–22} Likewise, two-plate DMF can be used to purify proteins from serum in a multistep process comprising precipitation, rinsing, and resolubilization.^{22,23} Ideally, digital microfluidics could be coupled with microchannels (as noted, microchannels are well-suited for chemical separation analysis) on a single platform for a fully integrated lab-on-a-chip.

In response to this challenge, we recently developed the first device architecture combining reactions and processing by digital microfluidics with separations in microchannels.²⁴ We called this method “hybrid microfluidics,” and it comprised a single-plate digital microfluidic device interfaced in a “side-on” configuration

with a network of microchannels. Using this preliminary design, we performed proof-of-concept experiments including on-chip fluorescent labeling of amines in cell lysate and enzymatic digestion of proteins, followed by separation of the products. Subsequent to our work, related methods were reported coupling sample processing by DMF to (non-microchannel) separations columns.^{25,26} Clearly, there is great enthusiasm for the combination of digital microfluidics and chemical separations.

Our preliminary hybrid microfluidic device²⁴ (Figure 1a) used the single-plate DMF configuration, which simplified device construction and operation. However, single-plate digital microfluidics suffers from a key limitation: the actuation forces are not sufficient to facilitate droplet splitting or dispensing from reservoirs. Thus, as reported in our initial work,²⁴ droplets were dispensed onto the device by pipet, which introduced substantial error into the technique. Evaporation is also a concern for this format, as droplets are directly exposed to the environment. Furthermore, the PDMS channel used in the initial design was not ideal, as this material suffers from well-known disadvantages²⁷ for lab-on-a-chip applications (e.g., surface adsorption of analytes, solvent compatibilities, etc.). Finally, in this side-on configuration,

(19) Cho, S. K.; Moon, H.; Kim, C.-J. *J. MEMS* **2003**, *12*, 70–80.

(20) Luk, V. N.; Wheeler, A. R. *Anal. Chem.* **2009**, *81*, 4524–4530.

(21) Chatterjee, D.; Ytterberg, A. J.; Son, S. U.; Loo, J. A.; Garrell, R. L. *Anal. Chem.* **2010**, *82*, 2095–2101.

(22) Jebrail, M. J.; Luk, V. N.; Shih, S. C. C.; Fobel, R.; Ng, A. H. C.; Yang, H.; Freire, S. L. S.; Wheeler, A. R. *J. Visualized Exp.* **2009**, *33*, doi: 10.3791/1603.

(23) Jebrail, M. J.; Wheeler, A. R. *Anal. Chem.* **2009**, *81*, 330–335.

(24) Abdelgawad, M.; Watson, M. W. L.; Wheeler, A. R. *Lab Chip* **2009**, *10*, 1046–1051.

(25) WIPO Patent 111432 A2, 2009.

(26) Gorbatsova, J.; Jaanus, M.; Kaljurand, M. *Anal. Chem.* **2009**, *81*, 8590–8595.

(27) Rolland, J. P.; Van Dam, R. M.; Schorzman, D. A.; Quake, S. R.; DeSimone, J. M. *J. Am. Chem. Soc.* **2004**, *126*, 2322–2323.

the DMF electrodes and the channel network share a common substrate, which limits the space available for droplet actuation electrodes.

Here, we introduce a new multilayer hybrid microfluidics configuration (Figure 1b), in which a digital microfluidic device is formed on a top substrate which is mated to a network of microchannels below. Although the fabrication of this type of device is more complex than the initial design, the new configuration has several substantial improvements. The most important advantage is the two-plate DMF configuration, which enables dispensing from reservoirs and splitting of droplets on-chip (reducing sample handling errors) and also limits evaporation. In addition, the new glass substrate is superior to the (previous) PDMS substrate, and the decoupling of the DMF and microchannel platforms in the new design allows for arbitrarily large DMF electrode patterns. In the following, we describe the implementation of this multilayer hybrid microfluidic device and present its application to sample processing and separations. We believe this will be an important step toward fully automated lab-on-a-chip methods suitable for a wide range of applications.

MATERIALS AND METHODS

Reagents and Materials. All chemicals, unless otherwise stated, were purchased from Sigma Aldrich (Oakville, ON) and used without further purification. Alexa Fluor 488 labeled bovine serum albumin (AF-BSA) was from Invitrogen-Molecular Probes (Eugene, OR) and food coloring dyes were from McCormick Canada (London, ON). Sodium borate and acetate buffers were dissolved in deionized water (diH_2O , 18 M Ω cm), filtered through Millipore nylon syringe filters (Billerica, MA, 0.2 μm pore dia.) and degassed by ultrasonication (5 min) prior to use. Materials required for device fabrication included Parafilm-M laboratory film (Pechiney Plastic Packaging, Menasha, WI) chromium pellets (Kurt J. Lesker Canada, Toronto, ON), parylene-C (Specialty Coating Systems, Indianapolis, IN), and Teflon-AF1600 (DuPont, Wilmington, DE).

Device Fabrication and Operation. Glass slides bearing a simple cross-pattern of microchannels (100 μm wide \times 20 μm deep; substrate 3 in Figure 2) thermally bonded to slides with drilled-hole (1.5 mm dia.) inlets (substrate 2 in Figure 2) were obtained from Caliper Life Science (Hopkinton, MA). The devices were then modified by patterning a digital microfluidic device (an array of chromium electrodes coated with Parylene-C and Teflon-AF) on top of substrate 2. As shown in Figure 2, the DMF design comprised thirteen driving electrodes (2.2 mm \times 2.2 mm) and three reservoir electrodes (3 \times 3 mm or 5 \times 5 mm) and was positioned such that one of the driving electrodes was adjacent to one of the inlets—this inlet served as the “digital-channel interface.”

The digital microfluidic device architecture was formed in the University of Toronto Emerging Communications and Technology Institute (ECTI) using methods described elsewhere^{22,23} with two modifications. First, prior to coating with chromium, the channel inlets were protected by inserting small plugs of Parafilm-M; after coating with chromium, the plugs were carefully removed. Second, after electrode patterning, the channels were inspected and rinsed with acetone and methanol, and the vertical inlets were sealed with dicing tape (Semiconductor Equipment Corp., Moorpark,

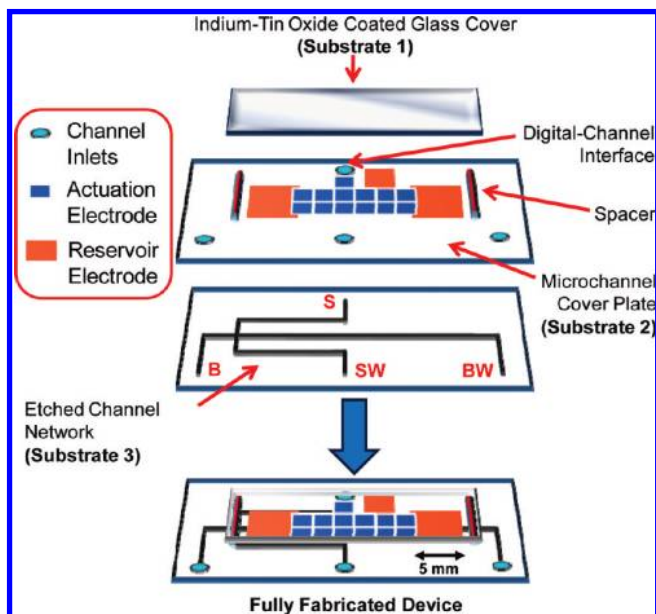


Figure 2. Exploded view of a multilayer hybrid microfluidic device. A two-plate digital microfluidic (DMF) structure is defined by substrates 1 and 2, and the network of microchannels is defined by substrates 2 and 3. In practice, the DMF architecture was fabricated on the top of preformed commercially available glass microchannel devices.

CA). After coating with Parylene-C and Teflon-AF the tape was removed.

After coating, hybrid devices were largely complete, save for the final preparation steps. Pipette tips were trimmed into pieces capable of holding $\sim 20 \mu\text{L}$ and were inserted into all of the microchannel access holes except for the digital-channel interface. Platinum wires were inserted into each of these reservoirs. At the digital-channel interface, a platinum wire was affixed such that it was flat on the surface of the top substrate, terminating in a hook that penetrated the access hole. Samples and reagents were pipetted into the DMF reservoirs, and a top plate (substrate 1 in Figure 2) comprising an indium–tin oxide (ITO) and Teflon-AF coated glass slide formed as described elsewhere^{22,23} was positioned on top of the device. The top plate was separated from the array of electrodes by spaces formed from four pieces of double-sided tape (280 μm total thickness). Finally, the network of microchannels was filled with separation buffer (20 mM or 100 mM borate buffer, pH 9.0, for on-chip dilutions or enzyme digests, respectively).

Device operation comprised two stages: sample processing by droplet actuation followed by chemical separation by electrophoresis. In the first stage, droplet actuation (i.e., dispensing, merging, mixing, and splitting) was implemented in two-plate format. Voltages for actuation of droplets were generated by applying an AC signal (20 kHz, 100–200 V_{rms}) originating from a function generator (Agilent, Santa Clara, CA) and high-voltage amplifier (Trek, Medina, NY). After sample processing in droplets (described in detail below) was complete, samples to be analyzed were driven to the digital-channel interface inlet for sampling into the microchannels below. In the second device operation stage (analysis by separation), DC voltages were applied at the sample inlet (S), sample waste outlet (SW), buffer inlet (B) and buffer waste outlet (BW) using a high voltage sequencer (LabSmith, Livermore, CA). Initially, the solution

in the droplet at the interface was driven through the injection cross by applying high voltage between S and SW ($S = 900$ V; $SW = 0$ V; $B = 650$ V; $BW = 850$ V). A plug of sample was then injected onto the separation column by switching voltage to drop between B and BW ($S = 500$ V; $SW = 500$ V; $B = 1000$ V; $BW = 0$ V).

Analytes were detected 3 cm downstream from the injection cross by LIF using an inverted microscope (Olympus IX-71) mated to an argon ion laser (Melles Griot, Carlsbad, CA). The 488 nm laser line (20 mW) was focused into the channel using an objective (60 X); the fluorescent signal was collected by the same lens and filtered optically (536/40 nm band-pass and 488 nm notch filter) and spatially (500 μ m pinhole), and imaged onto a photomultiplier tube (PMT, Hamamatsu, Bridgewater, NJ). PMT current was converted to a voltage using a picoammeter (Keithley Instruments, Cleveland, OH) and then collected using an A–D converter and a PC running a custom LabVIEW (National Instruments) program to generate electropherograms.

On-Chip Calibration Curves. To generate on-chip calibration curves, a droplet containing both rhodamine 123 and fluorescein (1 μ M each in 20 mM borate buffer, pH 9.0) was dispensed and merged with a second droplet containing only rhodamine (1 μ M) and mixed by moving the droplet across several electrodes. The mixed droplet (~ 0.5 μ M fluorescein and 1 μ M rhodamine) was then split into two subdroplets; one subdroplet was stored on the array while the other was driven to the interface and analyzed. The stored droplet was then merged and mixed with a third droplet of rhodamine (1 μ M), to create the next dilution (~ 0.25 μ M fluorescein and 1 μ M rhodamine). Again, this droplet was split, and one subdroplet was driven to the interface for analysis, while the other subdroplet was stored. Between each analysis, the remaining portion of the previous sample was removed by suction with a fine needle connected to a vacuum flask, without removing the DMF top-plate. The entire process (including all dilutions) required ~ 5 min including replenishing the buffers and samples.

After collecting electropherograms, peak areas were quantified using PeakFit (SeaSolve Software Inc., Framingham, MA). In each case, the peak area of fluorescein was measured relative to that of the internal standard, rhodamine 123. The resulting ratio was plotted as a function of fluorescein concentration to generate calibration curves. The variance of this method was probed by assessing the percent relative standard deviation (% RSD) from five replicates.

On-Chip Protein Digestion. A model protein, AF-BSA, was used to demonstrate the compatibility of the new device architecture with multistep sample processing. In each experiment, a droplet of AF-BSA (20 μ g/mL in DI water containing 0.1% wt. F-68) was dispensed, merged and mixed with a droplet containing either pepsin (1 mg/mL in 1 mM acetate buffer containing 0.1% wt. F-68, pH 4.5) or trypsin (1 mg/mL in 50 mM borate buffer containing 0.1% wt. F-68, pH 9.0). After droplet merging, the device was incubated (30 min) in a humidified chamber (a Petri dish containing a water-saturated wipe), after which the combined droplet was split and one subdroplet was delivered to the interface for analysis. Experiments included analysis of AF-BSA alone, AF-BSA digested by pepsin alone, AF-BSA digested by trypsin alone, and AF-BSA digested by pepsin followed by trypsin. Each

condition was repeated in triplicate. The entire process (including both digestion steps) required ~ 2 h including incubations.

RESULTS AND DISCUSSION

Device Fabrication and Operation. We have developed a new architecture mating digital microfluidics (useful for sample processing) to microchannels (useful for separations). The new multilayer hybrid devices were formed by creating a DMF device on the top surface of a commercially available glass device bearing a network of microchannels. An exploded view is shown in Figure 2—as depicted, the digital microfluidic device is defined by substrates 1 and 2, and the network of microchannels is defined by substrates 2 and 3. Critically, the new multilayer architecture facilitates manipulation of droplets in the two-plate format, allowing for dispensing from reservoirs and splitting of droplets on-chip. This represents a significant advance over the previous hybrid microfluidic device configuration²⁴ which relied on single-plate actuation (which is incompatible with on-chip dispensing and droplet splitting).

The new device was designed such that the two fluid manipulation paradigms—electrostatic droplet manipulation in the top layer and electroosmotic flow in the bottom layer—are orthogonal and independent. For the former, droplets were dispensed from reservoirs, merged, mixed, and split by applying a series of AC potentials to sequential driving electrodes. Adsorption of proteins and reagents from droplets onto device surfaces was minimized by the addition of pluronic as a buffer additive,²⁸ and droplet evaporation over extended incubation times was mitigated by storing devices in a humidified chamber.²⁹ For the latter, sample at the digital-channel interface was loaded and separated by applying DC voltage to drive electroosmotic flow (EOF) through the channels. Channels and reservoirs were filled prior to actuation of droplets and were cleaned and refilled after performing electrophoretic separations.

As shown in Figure 2, the central feature of this design is a vertical digital-channel interface formed at the intersection of a DMF electrode and one of the drilled-hole channel inlets. Thus, in this scheme, droplets are manipulated on the top of the device, and are subsequently transferred to microchannels on the bottom of the device through the interface. This process is depicted in Figure 3. As shown, a droplet is actuated on the array of electrodes (not visible in the perspective of Figure 3) such that it approaches the digital-channel interface. As the droplet reaches the inlet, it spontaneously wets the exposed glass, settling into the bottom of the hole. In this design, unit droplet volumes (~ 3 μ L) were chosen to approximate the volume bounded by the hole (2 mm diam., 1 mm deep), but this is not a requirement for operation.

In initial work, the design and fabrication protocol for hybrid microfluidic devices was optimized to address two challenges: droplet transition into the network of microchannels, and protection of the channel network during cleanroom processing. For the former challenge, we found that reliable sample transfer into the interface hole required that the actuation electrode (2.2 \times 2.2 mm) be aligned to partially overlap with the vertical hole (2 mm diam.). In initial experiments, we found that if the electrode and

(28) Luk, V. N.; Mo, G. C.; Wheeler, A. R. *Langmuir* **2008**, *24*, 6382–6389.

(29) Barbulovic-Nad, I.; Yang, H.; Park, P. S.; Wheeler, A. R. *Lab Chip* **2008**, *8*, 519–526.

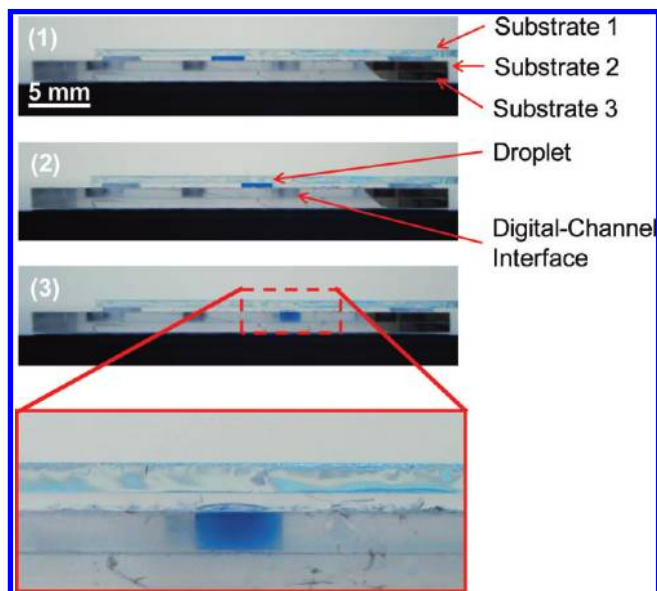


Figure 3. Series of images from a movie (side-view) depicting sample transfer from the digital microfluidic platform (above) to the network of microchannels (below). As the droplet (colored blue for visualization) approaches the digital-channel interface (a drilled hole in the glass), it spontaneously wets and settles into the hole. A magnified image of the droplet settled in the inlet is shown in the bottom panel.

hole do not overlap, the droplet will not contact the exposed glass; however, if the electrode and hole overlap too much, the electrode will not be sufficiently attractive to the droplet. In the final design, the interface electrode was patterned such that it overlapped the interface access hole by ~ 1 mm, which facilitated reliable droplet transfer. For the latter challenge, we found that protection of the channels during electrode patterning and coating was necessary to prevent channel clogging. During metal deposition and photoresist coating, channel inlets were protected with plugs of parafilm, which is easy to mold and forms a tight seal. Paraffin was also explored as a channel protectant;³⁰ however, the high temperatures required for metal deposition and photoresist curing was observed to cause the paraffin to melt. During Parylene-C and Teflon-AF coating, we found that it was best to protect channels by covering the inlets with dicing tape. This was particularly important at the digital-channel interface—the tape must be carefully positioned such that the electrode is exposed but the hole is covered. Parafilm plugs were not used for this step because the conformal Parylene-C coating makes extraction of the plugs difficult, leading to peeling or blistering of the dielectric layer.

An additional challenge for device operation was optimization of sample/buffer volumes. In microchannel electrophoresis, large reservoir volumes are often used to limit the effects of buffer depletion and evaporation, which can lead to unpredictable EOF rates. Moreover, it is often advisable to match the fluid heights in reservoirs to avoid siphoning and unwanted pressure-driven flows.⁷ Unfortunately, in the new hybrid device design, the sample volume is limited (e.g., in the device described here, the sample volume is formed from a $3 \mu\text{L}$ droplet). In response to this challenge, we adopted a strategy in which large volumes ($15 \mu\text{L}$)

were used for buffer, buffer waste, and sample waste reservoirs, and a small volume ($3 \mu\text{L}$ droplet) for the sample. Pressure-driven flow toward the sample inlet is observed under these conditions; however, it is predictable, and the voltages for EOF loading and electrokinetic separations were chosen to compensate for the pressure-driven flow. In the future, we may use channel restrictions³¹ or porous polymer plugs³² to mitigate the effects of siphoning further.

On-Chip Calibration Curves. The unique hybrid structure of the device architecture reported here makes it straightforward to integrate sample preparation with chemical separations. As shown in Figure 4, droplets can be dispensed from reservoirs (frame 2), merged (frame 3), mixed (frames 3–4) and split to form subdroplets (frames 4–5). Droplet dispensing and splitting are particularly welcome capabilities, as the initial hybrid microfluidic design²⁴ (relying on single-plate DMF) was incapable of these operations. In the design reported here, after completion of processing, samples can be transferred to the network of channels below for analysis (frame 6). To illustrate this capacity, we used the new method to create a set of calibration standards on the digital platform with in-line analysis by electrophoretic separations.

Serial dilutions were formed by merging a droplet containing both analyte (fluorescein) and internal standard (rhodamine 123) with a droplet of diluent (buffer containing internal standard only). Thorough mixing (by moving the merged droplet in a circular pattern for several seconds³³) produced a droplet with a $2\times$ dilution of analyte. This droplet was split (as in Figure 4, frames 4–5), and one daughter droplet was analyzed by electrophoresis and LIF, and the other daughter droplet was stored for further processing. Subsequent mixing of the stored droplet with another droplet of diluent resulted in a product droplet with $4\times$ -diluted analyte concentration. Note that this type of process, which includes dispensing multiple droplets from the reservoirs and splitting droplets on-chip, is made possible by the two-plate configuration used. Such operations were not possible with the previous design.²⁴ The devices used in this experiment were designed with equal-sized electrodes, which allowed for a maximum of a $4\times$ dilution of stock analyte. In the future, different dilutions could be implemented by using devices to mix and merge droplets dispensed onto different sized electrodes.

Figure 5 summarizes the results of replicate ($n = 5$) electrophoretic analyses of the serial dilution experiment. Figure 5a is a series of representative electropherograms for a dilution curve set (i.e., undiluted stock, first dilution and second dilution). Both the analyte and the internal standard are fully baseline resolved and peak area was used as the calibration metric. A calibration curve (Figure 5b) was generated by plotting the ratio of analyte peak area (A_A) to that of the internal standard (A_{IS}) as a function of analyte concentration. The precision in each measurement (RSD = 2.9%, 3.7%, and 7.4% for the stock, first dilution, and second dilution, respectively) and the correlation coefficient ($R^2 = 0.9937$) demonstrates that the method is reproducible and linear. As expected, the precision of the new method was

(31) Siegrist, J.; Gorkin, R.; Clime, L.; Roy, E.; Peytavi, R.; Kido, H.; Bergeron, M.; Veres, T.; Madou, M. *Microfluid. Nanofluid.* **2009**, *9*, 55–63.

(32) Fintschenko, Y.; Arnold, D.; Peters, E.; Svec, F.; Frechet, J. *Proc. SPIE* **1999**, *3877*, 202–209.

(33) Paik, P.; Pamula, V. K.; Fair, R. B. *Lab Chip* **2003**, *3*, 253–259.

(30) Kelly, R. T.; Pan, T.; Woolley, A. T. *Anal. Chem.* **2005**, *77*, 3536–3541.

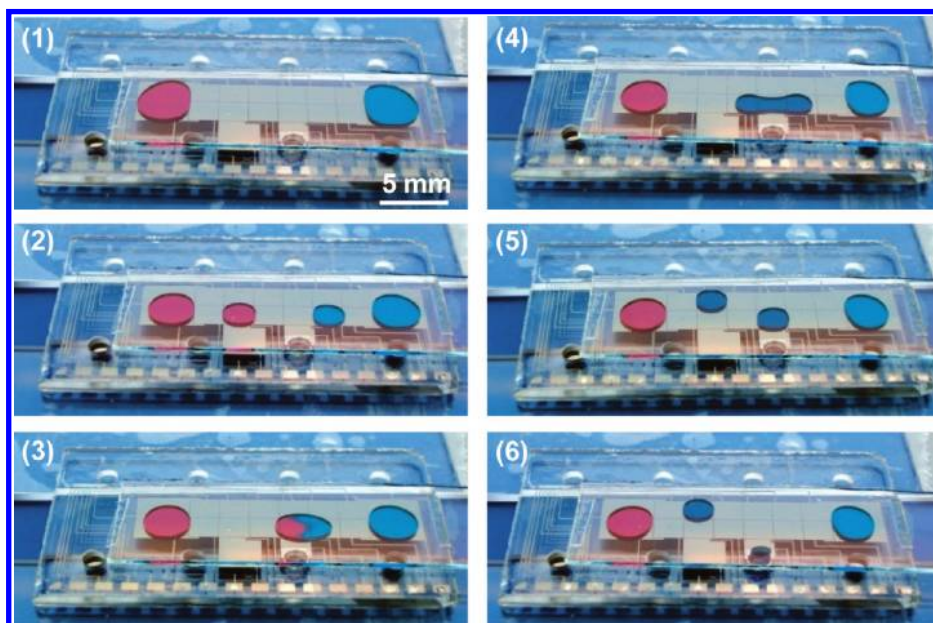


Figure 4. Series of images from a movie (top-view) depicting droplet manipulation on the hybrid microfluidic device. Devices were capable of all basic DMF operations: dispensing (frames 1–2), merging (frame 3), mixing (frames 3–4) and splitting (frames 4–5). Processed droplets were then delivered to the vertical interface to access the channels below (frame 6). Red and blue dyes were added for visualization.

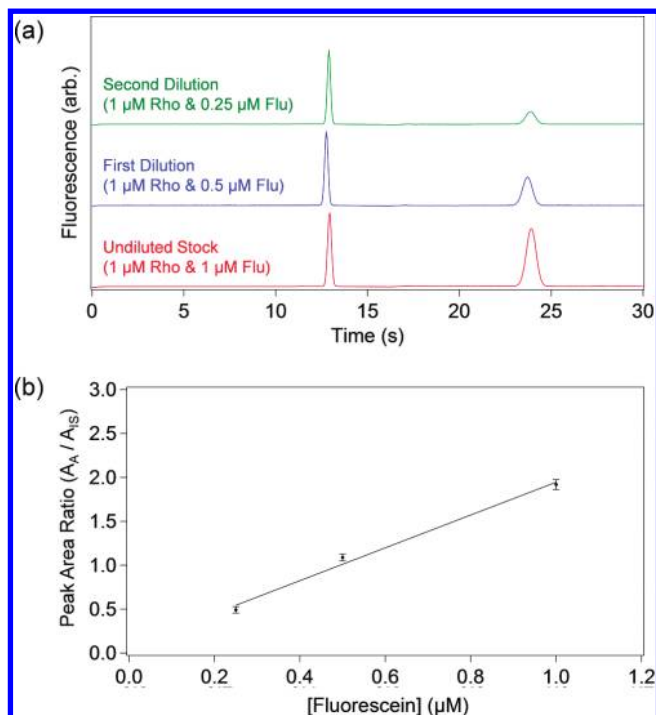


Figure 5. Data generated from on-chip serial dilutions and analysis. (a) Representative electropherograms of analyte, fluorescein (Flu) and internal standard, rhodamine 123 (Rho) from an undiluted stock, first dilution and second dilution (offset vertically for clarity). (b) Calibration curve for the ratio of peak area of analyte (A_A) to that of internal standard (A_{IS}) from five replicate analyses. Error bars are ± 1 SD.

improved relative to that of the side-on design (i.e., in analogous experiments, 2.9% RSD was observed for the current design and 6.7% RSD was observed for the side-on design²⁴). Efficiency for the separation using the new method (1.1×10^6 plates/m for rhodamine 123) was also very high, and represents an improvement over what was reported for the previous design²⁴ (4.7×10^5 plates/m for rhodamine 123). The improvement can

be attributed to the channel materials, as PDMS (used in the previous design) is known to contribute to band broadening relative to glass (used in the current design).

Multistep Protein Processing. Analysis of complex samples often requires the combination of multistep sample processing followed by analysis by separations. A well-known example is shotgun proteomics,⁶ in which samples are exposed to a rigorous sample processing regimen and then separated by HPLC. A key step in this method is enzymatic digestion of proteins into constitutive peptides which are easier to handle and analyze. In fact, this step is so important, that samples are often digested serially with multiple enzymes that cleave at different amino acid residues.⁶ Here, we used the new multilayer hybrid microfluidic device to integrate digestion by multiple enzymes followed by separations. In this work, a model analyte (fluorescently labeled bovine serum albumin, AF-BSA) was digested by pepsin (which cleaves at Phe, Tyr, and Trp) and trypsin (which cleaves Arg and Lys). All solution processing was implemented on the DMF platform, and the resulting processed samples were delivered to the digital-channel interface for analysis by microchannel electrophoresis.

AF-BSA was analyzed in three states: undigested, digested with pepsin (30 min), and digested with pepsin (30 min) followed by digestion with trypsin (30 min each). (AF-BSA digested with trypsin-only was also analyzed, but is not shown.) As shown in Figure 6, each enzyme produces a unique series of peaks in the resulting electropherograms. Pepsin selectively cleaves at aromatic residues (Trp, Tyr, and Phe), resulting in multiply charged peptides. The resulting electropherograms (middle trace in Figure 6) include several peaks that elute at a range of times relative to the AF-BSA reactant. From this data, the digestion appears to be complete, as the peak for AF-BSA ($t = 58$ s) is no longer observed. Trypsin selectively cleaves at basic residues (Lys and Arg), resulting in a reduction of multiply charged peptides from the pepsin digestion. Thus, in these electropherograms (top trace in

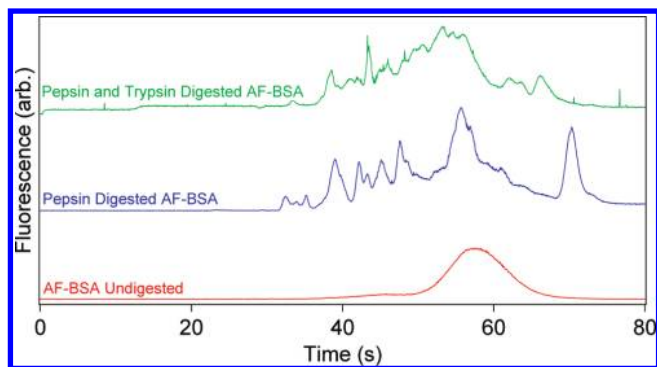


Figure 6. Multistep processing of a model protein. AF-BSA was subjected to enzymatic digestion by two proteolytic enzymes; pepsin and trypsin. The three electropherograms (offset vertically for clarity) represent (1) undigested AF-BSA ($20 \mu\text{g/mL}$), (2) AF-BSA digested by pepsin (30 min), and (3) AF-BSA digested by pepsin followed by trypsin (30 min each).

Figure 6), a new series of peaks is observed, with the peptides eluting closer together.

The small footprint of the commercial microchannel devices ($35 \times 20 \text{ mm}$) used here limited the size of the DMF array to a few electrodes. In the future, we plan to fabricate larger devices capable of supporting DMF platforms that can manipulate up to 10 different reagents²² to integrate on-chip protein precipitation²³ and sample reduction, alkylation, and digestion.²⁰ Note that such operations require two-plate actuation (as in the multilayer configuration reported here) and are incompatible with single-

(34) Watson, M. W. L.; Mudrik, J. M.; Wheeler, A. R. *Anal. Chem.* **2009**, *81*, 3851–3857.

(35) Freire, S. L. S.; Yang, H.; Wheeler, A. R. *Electrophoresis* **2008**, *29*, 1836–1843.

plate actuation (as in the side-on configuration²⁴ described previously). In the long term, we anticipate that integration of such techniques with microchannel chromatography³⁴ and nanoelectrospray mass spectrometry³⁵ will form a powerful new tool for application to shotgun proteomics and many other applications.

CONCLUSIONS

We introduced a new multilayer hybrid microfluidic device architecture, bearing a digital microfluidic module on the top of the device and a network of microchannels below. In such devices, droplets are dispensed from reservoirs, merged, mixed, and split on the top layer, and are subsequently transferred to microchannels on the bottom of the device through a vertical interface. To validate the capabilities of the new method, we implemented an on-chip serial dilution experiment, as well as multistep enzymatic digestion. Given the myriad applications requiring preprocessing and chemical separations, the two-layer hybrid digital-channel format has the potential to become a powerful new tool for micrototal analysis systems.

ACKNOWLEDGMENT

The authors thank the Natural Sciences and Engineering Council (NSERC), the Canadian Cancer Society (CCS), and Eli Lilly and company for financial support. M.W.L.W. thanks the Ontario Graduate Scholarship program and A.R.W. thanks the CRC for a Canada Research Chair. M.W.L.W. and M.M.J. contributed equally to this work.

Received for review May 26, 2010. Accepted July 1, 2010.

AC101379G